

## Supporting information for:

### AACVD synthesis and gas sensing properties of nickel oxide nanoparticle decorated tungsten oxide nanowires

Èric Navarrete<sup>1</sup>, Carla Bittencourt<sup>2</sup>, Polona Umek<sup>3</sup>, Eduard Llobet<sup>\*1</sup>

<sup>1</sup>MINOS-EMaS, Universitat Rovira i Virgili, Avda. Països Catalans, 26, 43007 Tarragona, Spain

<sup>2</sup>Chimie des Interactions Plasma – Surface (ChIPS), Research Institute for Materials Science and Engineering, Université de Mons, Avenue Copernic 1, 7000 Mons, Belgium

<sup>3</sup>Jožef Stefan Institute, Jamova cesta 39, 10000 Ljubljana, Slovenia.

\*Correspondence: eduard.llobet@urv.cat; Tel.: +34 977 558 502

#### 1. Results employing the one-step deposition approach

At first the AA-CVD process was performed in one step mixing both the tungsten oxide and the nickel oxide organic precursors in the same solution and subsequently deposited. The results obtained through this one step procedure revealed a non-homogeneous nickel deposition.

The following table displays the average chemical composition of nickel doped sensors resulting from running the 1 step procedure. This composition has been estimated by XPS. Low-concentration loading (LC) corresponds to using 2.5 mg of Ni precursor and high-concentration loading (HC) corresponds to using 5 mg of Ni precursor.

**Table S1.** Average composition in weight percentage for the Ni-loaded sensing layers obtained employing the 1-step deposition approach.

	<b>W</b>	<b>O</b>	<b>Ni</b>
1ST Ni/LC	<b>22.0</b>	<b>76.5</b>	<b>1.5</b>
	<b>W</b>	<b>O</b>	<b>Ni</b>
1ST Ni/HC	<b>22.4</b>	<b>75.8</b>	<b>1.9</b>

The amount of nickel loading is rather low and does not differ substantially for LC and HC samples. In addition, the morphology of the Ni-loaded samples is not the expected. Even though tungsten oxide nanowires are obtained, in many regions of the samples an unexpected cauliflower shaped morphology appears as revealed by SEM (see the micrographs below in Figure S1). The EDX analysis of the chemical composition of these abnormal microstructures indicates that they contain tungsten and nickel. Considering the poor, inefficient results of Ni loading and the abnormal microstructure of the resulting films, the single step approach was discarded and a two-step approach implemented.



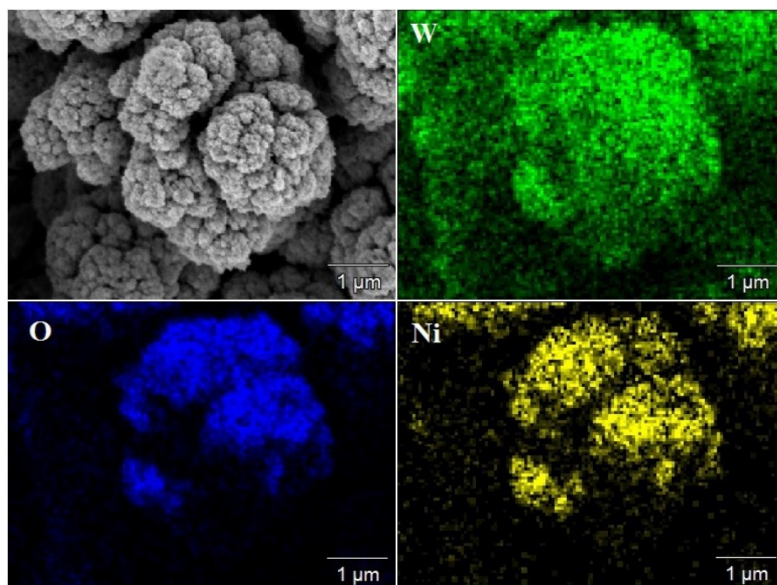


**Figure S1.** A SEM image and the corresponding elemental maps (W – green, O – blue and Ni – yellow) for the cauliflower structures present in Ni-loaded samples obtained via the single step deposition approach.

## 2. Additional results on the two-step deposition approach

Sensors were characterized by EDX as qualitative and XPS as quantitative techniques, in order to confirm the presence of nickel. The following figure shows the results of EDX performed on a Ni-loaded tungsten oxide nanowire sample obtained via a two-step deposition approach. EDX confirms the presence of Ni. The Pt peaks in the EDX spectrum correspond to the electrodes of the transducer onto which the gas sensitive film is deposited.

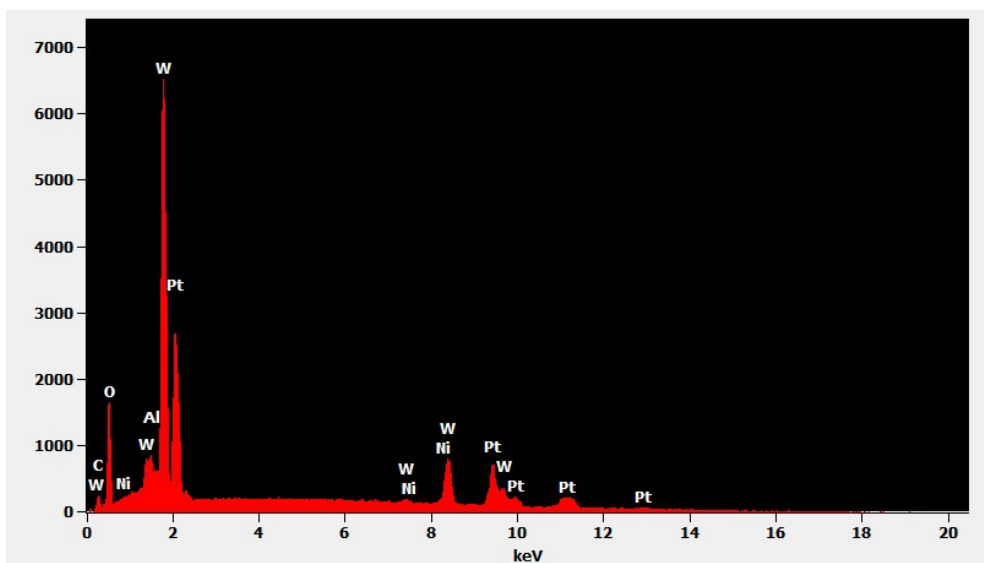


**Figure S2.** EDX results for a Ni/HC sensor.



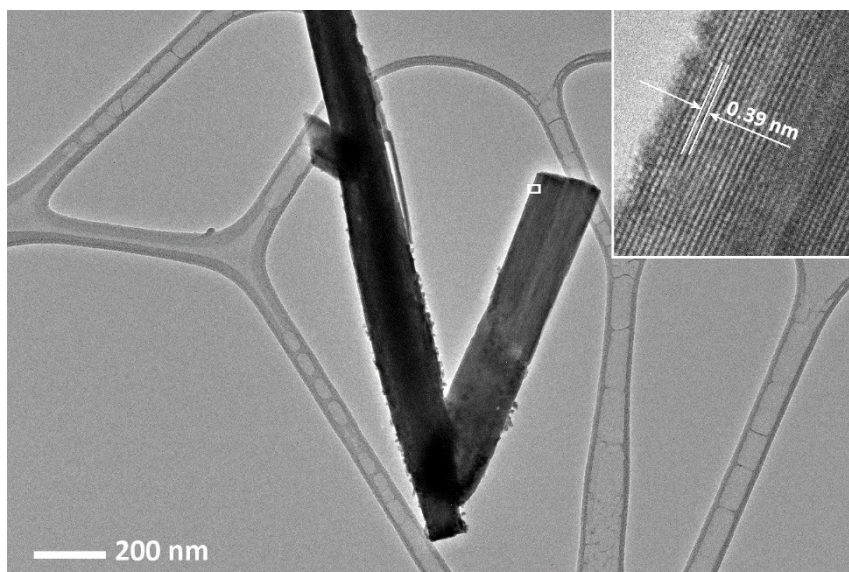


**Figure S3.** SEM micrograph of the Ni/LC sample. The HRTEM inset shows that the  $\text{WO}_3$  nanorod is crystalline. The d-spacing between lattice fringes in the inset is 0.39 nm corresponding to (002) planes in  $\text{WO}_3$  with triclinic structure (JPCDS 71-0305).

### 3. Response times

Tables S2 and S3 summarize the response times for pure and Ni-loaded tungsten oxide sensors. The response time  $t_{90}$  indicates the time needed for the sensor resistance to reach 90% of its steady state value upon a sudden change in gas concentration. Response times decrease when the operating temperature increases, as it could be expected. Despite the fact that the fastest responses are obtained at 250 °C, this operating temperature it is not always the optimal for achieving the highest response.

**Table S2.** Case of pure  $\text{WO}_3$  sensor. Average  $t_{90}$  response for each gas at different temperatures in seconds.  $t_{90}$  values appear in bold when they correspond to the operating temperature in which sensor response is maximal.

$\text{WO}_3$	150 °C	200 °C	250 °C
$\text{CH}_4 - 20 \text{ ppm}$	--	450	<b>255</b>
<b>Ethanol – 20 ppm</b>	<b>832</b>	450	255
$\text{NO}_2 - 10 \text{ ppm}$	<b>650</b>	325	272
$\text{H}_2\text{S} - 50 \text{ ppm}$	<b>158</b>	88	119



**Table S3.** Case of Ni/HC sensor. Average t90 response for each gas at different temperatures in seconds. t90 values appear in bold when they correspond to the operating temperature in which sensor response is maximal.

Ni/HC	150 °C	200 °C	250 °C
CH <sub>4</sub> – 20 ppm	--	363	<b>199</b>
Ethanol – 20 ppm	848	494	<b>149</b>
NO <sub>2</sub> – 10 ppm	<b>1720</b>	1210	568
H <sub>2</sub> S – 50 ppm	514	90	<b>88</b>

#### 4. H<sub>2</sub>S and layer degradation

It is well known that hydrogen sulfide is a compound that poisons metal oxide gas sensors and results in fast aging of the sensing films. The acidity of H<sub>2</sub>S leads to a corrosion of the structures, altering the original morphology of the gas sensitive films. This effect is clearly visible after several hours of operation at 250 °C and under high hydrogen sulfide concentrations (i.e. 50 ppm). As a result the initially observed responsiveness degrades. This effect has been studied for the different gas-sensitive layers produced. Figure S4 shows that morphological changes are visible after the films are exposed continuously to 50 ppm of hydrogen sulfide at 250 °C. Some corrugation develops on the walls of the Ni-loaded tungsten oxide nanowires, indicative of a corrosion effect. Furthermore, XPS performed on aged samples indicates a clear reduction in the amount of Ni present on the surface of the nanomaterial. These results are summarized in Table S4. Finally, the effects of such degradation in the response towards hydrogen sulfide are shown in Figure S5. In this experiment the sensor is under and accelerated ageing under high concentration of hydrogen sulfide. During the first 9 hours of exposure to 50 ppm H<sub>2</sub>S at the different operating temperatures considered, response remains stable. After this period of time, if the sensor surface remains exposed to such a high concentration of hydrogen sulfide, response degrades. This effect is more evident at higher operating temperatures.



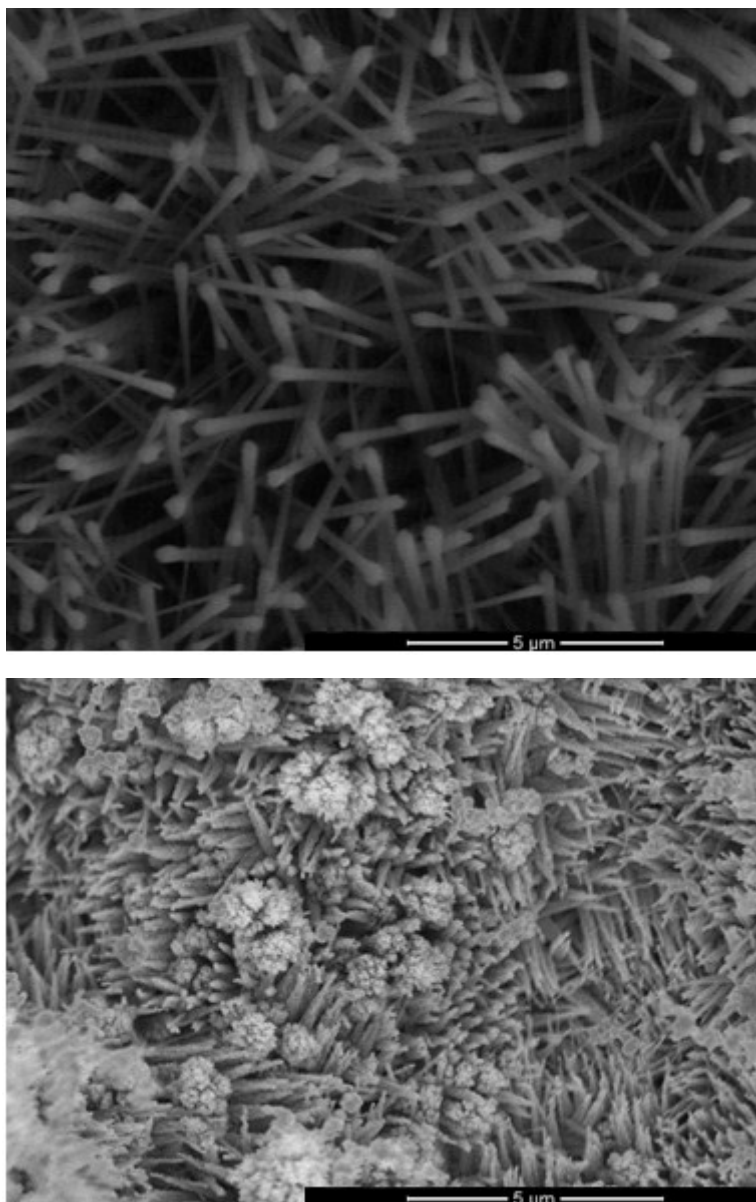


**Figure S4.** Unexposed sensing layer (upper panel) and H<sub>2</sub>S exposed sensing layer (lower panel).

**Table S4.** Sensing layer average composition in weight percentage after 18 hours of exposure to hydrogen sulfide, 50 ppm.

	<b>W</b>	<b>O</b>	<b>Ni</b>
<b>Ni/LC</b>	17.6	81.0	1.4
<b>Ni/HC</b>	18.0	80.0	2.0
<b>WO<sub>3</sub></b>	25.0	75.0	0



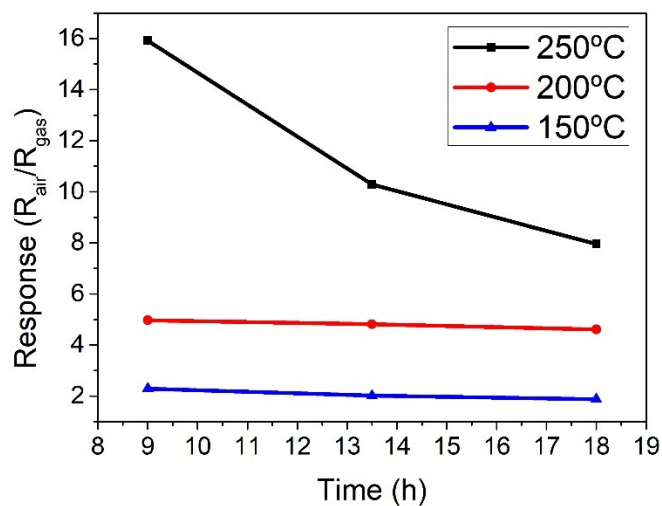


**Figure S5.** Degradation in sensor response after hours of exposure to 50 ppm H<sub>2</sub>S at the operating temperatures of 150 °C, 200 °C or 250 °C.

#### 5. Effect of nickel oxide loading on the response to hydrogen sulfide.

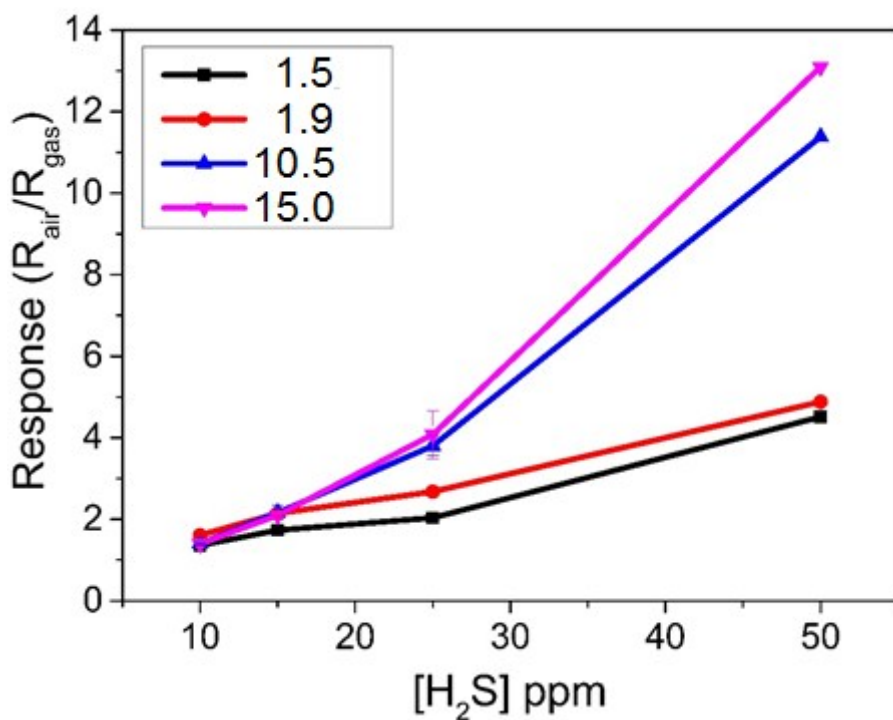


**Figure S6.** Response for different H<sub>2</sub>S concentrations of tungsten oxide nanowires sensors loaded with different amounts of nickel oxide. The legend indicates the atm. % of Ni as revealed by XPS. Sensors were operated at 250°C.